CUBIC SPLINE REFLECTANCE ESTIMATES

USING THE VIKING LANDER CAMERA MULTISPECTRAL DATA

Stephen K. Park and Friedrich O. Huck
NASA Langley Research Center

SUMMARY

A technique was formulated for constructing spectral reflectance estimates from multispectral data obtained with the Viking lander cameras. The output of each channel was expressed as a linear function of the unknown spectral reflectance producing a set of linear equations which were used to determine the coefficients in a representation of the spectral reflectance estimate as a natural cubic spline. The technique was used to produce spectral reflectance estimates for a variety of actual and hypothetical spectral reflectances.

INTRODUCTION

The Viking lander cameras (ref. 1) will return multispectral images of the Martian surface with four orders of magnitude higher resolution than has been previously obtained. It is desired to extract spectral reflectance curves from this data. However, the data are limited to 6 spectral channels and most of these channels exhibit out-of-band response.

It is inappropriate to generate a data point for each channel by associating a reflectance value with a distinct wavelength; this is particularly true for those channels with appreciable out-of-band response. It is unlikely that data points so constructed will lie on the true spectral reflectance curve, and that any method of fitting a curve to these points will adequately approximate the true reflectance.

Instead the output of each channel can be expressed as a linear integral function of the unknown spectral reflectance and the known solar irradiance, atmospheric transmittance, camera optical throughput, and channel responsivity. This produces 6 equations - one per channel - which can be used to determine the coefficients in a representation of the spectral reflectance as a natural cubic spline. In this paper the appropriateness of this technique is demonstrated by using it to produce accurate approximations to the true spectral reflectance of 8 materials felt likely to be present on the Martian surface and 16 hypothetical spectral reflectances chosen for illustrative purposes.

FORMULATION

Let $\rho(\lambda)$ denote the (unknown) spectral reflectance at wavelength λ of the material that is imaged by the Viking lander camera. Knowledge of $\rho(\lambda)$ is limited to 6 spectral samples. Except for a channel-dependent, multiplicative constant, which can be determined by a calibration using as reference a test chart on board the Viking lander (see ref. 2), these 6 spectral samples are given by b_i where

$$b_i = \int_0^\infty T_i(\lambda)\,\rho(\lambda)\,d\lambda \qquad i = 1,2,\ldots,6 \qquad (1)$$

The system transfer functions $T_i(\lambda)$ are given by

$$T_i(\lambda) = \frac{S(\lambda)\,\tau_a(\lambda)\,\tau_c(\lambda)\,R_i(\lambda)}{t_i} \qquad i = 1,2,\ldots,6$$

where $S(\lambda)$ is the solar irradiance, $\tau_a(\lambda)$ the atmospheric transmittance, $\tau_c(\lambda)$ the camera optical throughput, $R_i(\lambda)$ the channel responsivity, and t_i is a constant chosen so that

$$\int_0^\infty T_i(\lambda)\,d\lambda = 1 \qquad i = 1,2,\ldots,6$$

Plots of typical system transfer functions are shown in figure 1. Note specifically the appreciable out-of-band response of the Blue (i=1), IR2 (i=5), and IR3(i=6) channels. Note also that with the possible exception of the Green (i=2) channel, none of the system transfer functions are adequately approximated by an impulse function.

THE REFLECTANCE ESTIMATE AS A NATURAL CUBIC SPLINE

Equations (1) describe the relationship between the 6 multispectral samples $b_1, b_2, \ldots, b_6$ and the unknown reflectance $\rho(\lambda)$. These six equations can be used to produce a natural cubic spline estimate of $\rho(\lambda)$, denoted $\langle \rho(\lambda) \rangle$, where

$$\langle \rho(\lambda) \rangle = \sum_{j=0}^{7} x_j\, C(\lambda - \bar{\lambda}_j) \qquad (2)$$

The 8 knots $\bar{\lambda}_0, \bar{\lambda}_1, \ldots, \bar{\lambda}_7$ are chosen to be equally spaced and located at the wavelengths

$$\bar{\lambda}_j = .33 + j\Delta \qquad j = 0,1,2,\ldots,7$$

where the spacing is $\Delta = .12\ \mu m$. Recall that each cubic spline basis function $C(\lambda - \bar{\lambda}_j)$ is a bell-shaped curve centered at the knot $\bar{\lambda}_j$ and defined by $C(\lambda)$ where

$$C(\lambda) = \begin{cases} 2/3 - \left|\frac{\lambda}{\Delta}\right|^2 + \frac{1}{2}\left|\frac{\lambda}{\Delta}\right|^3 & |\lambda| \leq \Delta \\ \frac{1}{6}\left(2 - \left|\frac{\lambda}{\Delta}\right|\right)^3 & \Delta < |\lambda| < 2\Delta \\ 0 & |\lambda| \geq 2\Delta \end{cases}$$

The coefficients $x_0, x_1, \ldots, x_7$ are to be determined.

It is desirable to impose the natural boundary conditions $\langle \rho(\lambda) \rangle'' = 0$ at the knots $\bar{\lambda}_1$ and $\bar{\lambda}_6$. These two conditions give rise to the equations

$$x_0 - 2x_1 + x_2 = 0 \tag{3a}$$

and

$$x_5 - 2x_6 + x_7 = 0 \tag{3b}$$

The remaining six equations which determine the 8 coefficients are obtained by requiring the estimate $\langle \rho(\lambda) \rangle$ and actual reflectance $\rho(\lambda)$ to have indistinguishable camera multispectral responses (ref. 2), i.e.,

$$\int_0^\infty T_i(\lambda) \langle \rho(\lambda) \rangle \, d\lambda = \int_0^\infty T_i(\lambda)\, \rho(\lambda)\, d\lambda \qquad i = 1,2,\ldots,6 \tag{4}$$

This produces the six equations

$$\sum_{j=0}^{7} a_{ij}\, x_j = b_i \qquad i = 1,2,\ldots,6 \tag{5}$$

where b_i is given by equation (1) and

$$a_{ij} = \int_0^\infty T_i(\lambda)\, C(\lambda - \bar{\lambda}_j)\, d\lambda \tag{6}$$

To summarize, a natural cubic spline reflectance estimate corresponding to the multispectral sample $b_1, b_2, \ldots, b_6$ can be produced as follows:

(i) evaluate the $6 \times 8 = 48$ coefficients a_{ij} given by equation (6)

(ii) determine the 8 coefficients x_j by solving equations (3a), (3b), and (5)

(iii) form the estimate $<\rho(\lambda)>$ given by equation (2)

The estimate constructed in this manner reduces to an interpolating spline in the idealized situation where each system transfer function can be represented as an impulse function. To see this suppose that

$$T_i(\lambda) = \delta(\lambda - \lambda_i) \qquad i = 1,2,\ldots,6$$

where the impulse system transfer functions occur at the discrete wavelengths $\lambda_1, \lambda_2, \ldots, \lambda_6$. In this special case

$$b_i = \int_0^\infty \delta(\lambda - \lambda_i)\, \rho(\lambda)\, d\lambda = \rho(\lambda_i) \qquad i = 1,2,\ldots,6$$

and

$$a_{ij} = \int_0^\infty \delta(\lambda - \lambda_i)\, C(\lambda - \bar{\lambda}_j)\, d\lambda = C(\lambda_i - \bar{\lambda}_j)$$

so that $<\rho(\lambda)>$ is the (unique) natural cubic spline which interpolates the spectral reflectances $\rho(\lambda_1), \rho(\lambda_2), \ldots, \rho(\lambda_6)$.

RESULTS

Reflectance estimates were computed for 8 materials felt likely to be present on the Martian surface and for 16 hypothetical spectral reflectances chosen for testing and illustrative purposes. These estimates are presented in figures 2, 3, and 4. In each case the actual spectral reflectance is shown as a sequence of 71 discrete points (circles) in the wavelength range $.4 \leq \lambda \leq 1.1\ \mu m$ and the corresponding estimate is shown as a continuous curve. For each of the spectral reflectances the corresponding multispectral sample $b_1, b_2, \ldots, b_6$ was calculated from equation (1) using a 71 point Simpson's Rule. The coefficients a_{ij} were calculated in the same manner from equation (6) assuming each system transfer function to be zero outside the effective range of the camera photosensor arrays, namely $.4 \leq \lambda \leq 1.1\ \mu m$.

Figure 2 illustrates the reflectance estimates for the 8 materials felt likely to be present on the Martian surface. For those 5 simple reflectances (i.e., pinacetes 5 and 28A, Syrtis Major, augite, and average Mars) the estimates are excellent. For the 3 more complex reflectances (i.e., limonite, hypersthene, and olivine) the estimates are very good. The dominant features are reproduced; however, due to the undersampling inherent with just 6 channels, small period features are lost. Note particularly that the dominant absorption band (at $\lambda \approx .93\ \mu m$) for hypersthene is quite accurately estimated.

Figure 3 illustrates the reflectance estimates for 8 hypothetical spectral reflectances. The first 4 of these spectral reflectances (3a, 3b, 3c, and 3d) are very smooth and the corresponding estimates are almost exact. The next four (3e, 3f, 3g, and 3h) are not smooth but the estimates remain good. Note specifically that the pronounced minima in 3e and 3f are accurately reproduced. Note also in 3g the characteristic oscillation exhibited by the natural cubic spline in the neighborhood of a large slope. In 3h the loss of small period features is again evident.

Figure 4 illustrates the reflectance estimates for 8 additional hypothetical spectral reflectances. All 8 of these are of the form

$$\rho(\lambda) = .25 + .2 \sin \pi \left(\frac{\lambda - \alpha}{\beta} \right) \tag{7}$$

where the parameters α, β have the values:

	figure 4							
	a	b	c	d	e	f	g	h
α	.4	.275	.4	.31	.4	.33	.4	.35
β	.25	.25	.18	.18	.14	.14	.1	.1

As the period becomes shorter (i.e., as β decreases), the quality of the reflectance estimates deteriorates. This is particularly evident in the sequence 4a, 4c, 4e, 4g and less evident in the sequence 4b, 4d, 4f, 4h. It is also true that the quality of the estimate is affected by the location of dominant spectral reflectance features relative to the location of the system transfer functions. This is illustrated by figures 4e and 4f where the spectral reflectances differ only by a shift of .07 μm while the corresponding estimates differ dramatically. Figure 4g is a clear demonstration of aliasing whereby a short period harmonic spectral reflectance curve has a reflectance estimate which is nearly harmonic but with a larger (false) period.

CONCLUDING REMARKS

A technique was formulated for constructing natural cubic spline spectral reflectance estimates from multispectral data obtained with the Viking lander camera. Using this technique it was demonstrated that smooth, simple spectral reflectance curves can be estimated almost exactly. For more complex spectral reflectance curves, large period features can be faithfully reproduced; small period features are lost due to the undersampling inherent with the limited number of spectral channels. The technique completely compensates for system transfer functions with irregular shapes and appreciable out-of-band transmittance. Moreover the technique should be a valuable aid in selecting the number of spectral channels and their responsivity shapes when designing a multispectral imaging system. This design approach would prove to be of value especially if spectral reflectance properties of interest are known a priori and if the transfer function shapes are desired to be broad to obtain good signal-to-noise ratios.

REFERENCES

1. Huck, F. O.; McCall, H. F.; Patterson, W. R.; and Taylor, G. R.: The Viking Mars Lander Camera. Space Science Instrumentation, Vol. 1, 1975, pp. 189-241.

2. Park, S. K.; and Huck, F. O.: A Spectral Reflectance Estimation Technique for the Viking Lander Camera Multispectral Data. NASA TN D-8292, 1976.

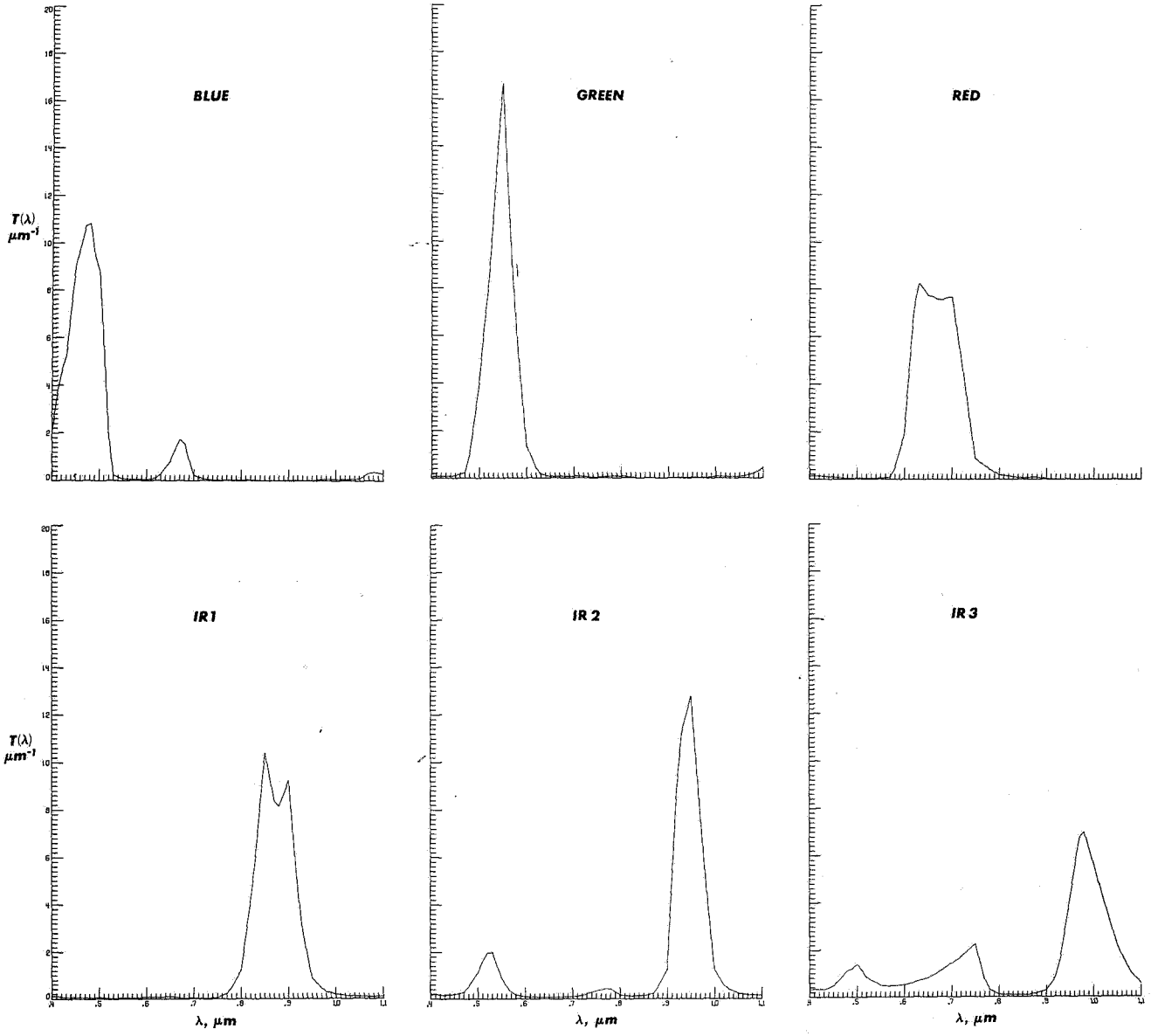

Figure 1.- Typical system transfer functions.

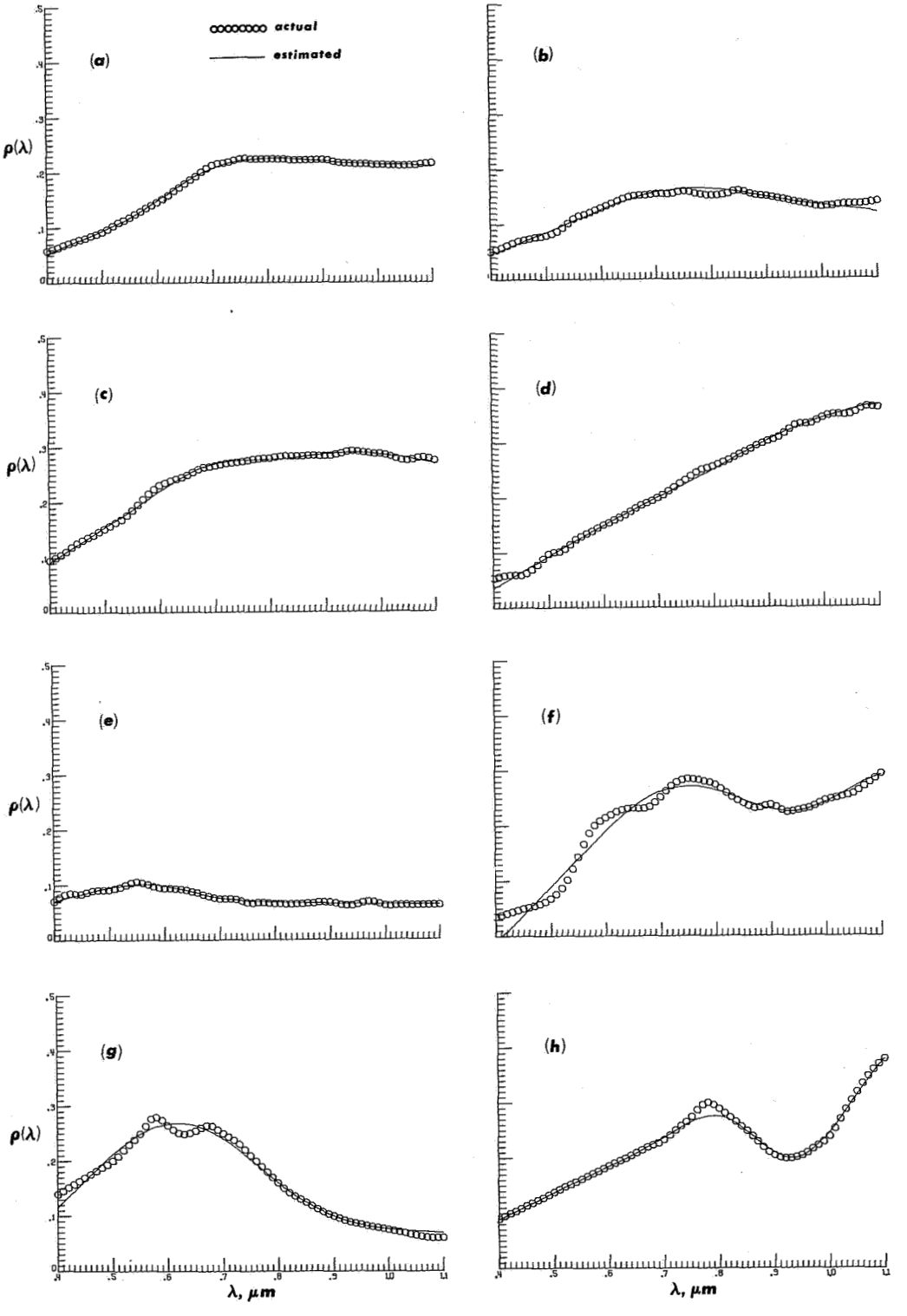

Figure 2.- Spectral reflectance estimates for (a) average Mars, (b) Syrtis Major, (c) pinacetes 5, (d) pinacetes 28A, (e) augite, (f) limonite, (g) olivine, and (h) hypersthene.

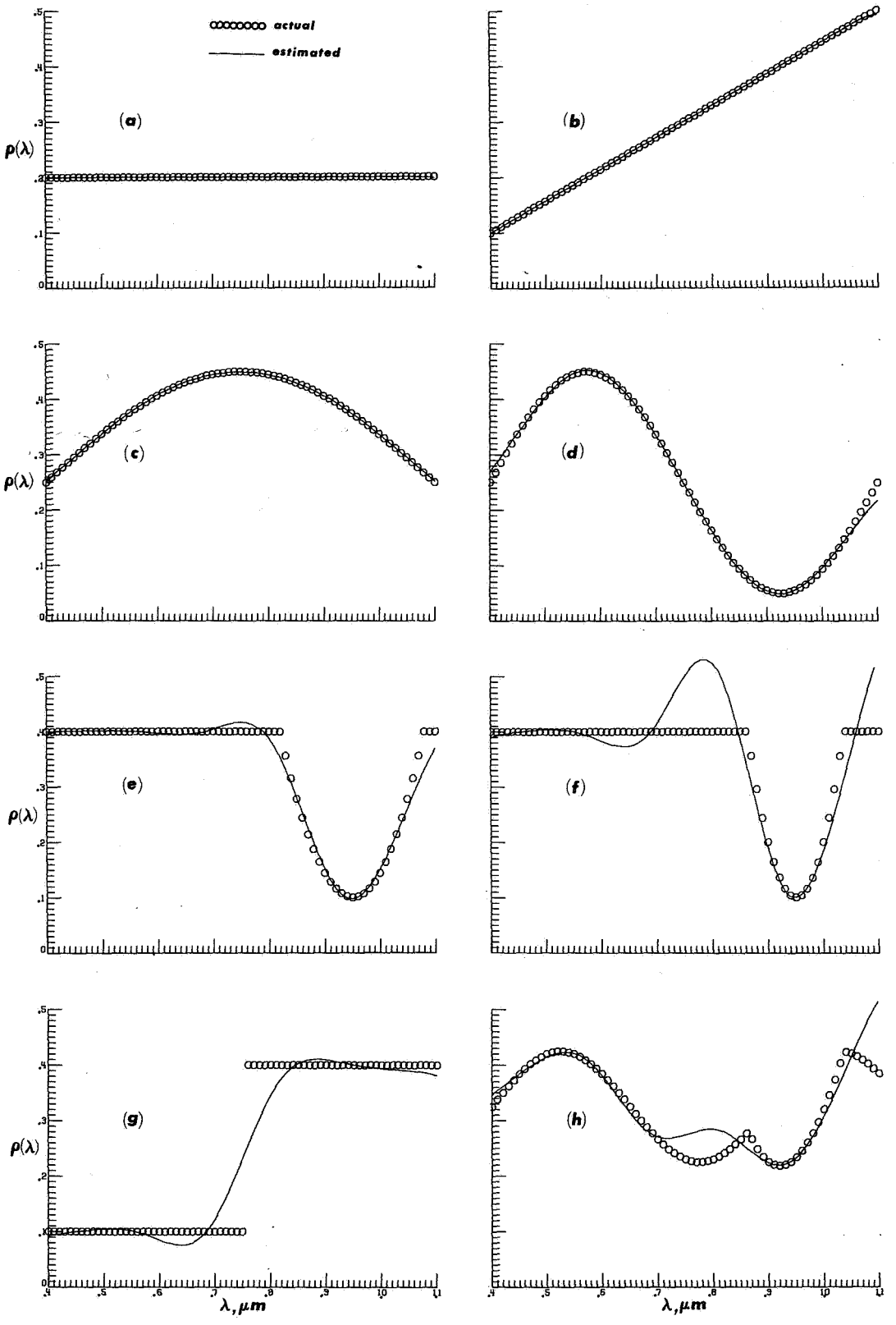

Figure 3.- Estimates for eight hypothetical spectral reflectances.

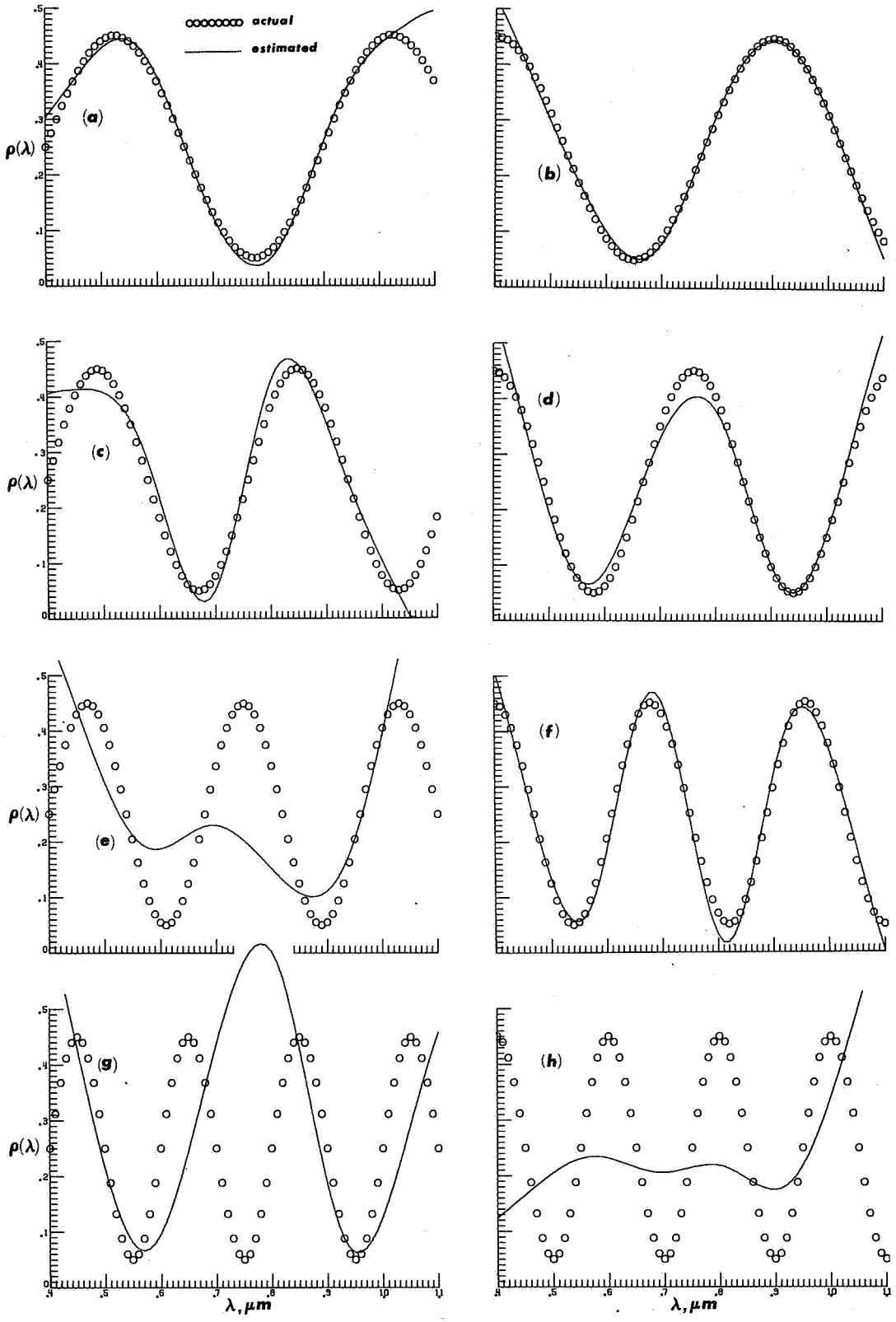

Figure 4.- Estimates for eight hypothetical spectral reflectances of the form given by equation (7).